



UNIVERSITY
OF APPLIED SCIENCES
UPPER AUSTRIA

BACHELOR MAJOR
AUTOMATION ENGINEERING

3D HIGH SPEED FILMING

As BACHELOR 1 THESIS submitted

to achieve the 5th semester

Bachelor of Science

of

Martin Kainrath

January 2018

Advised from

FH-Prof. DI Dr. Peter Zeller

Prof. John Renie Ph.D.

Sworn declaration

Wels Campus

I hereby declare that I prepared this work independently and without help from third parties, that I did not use sources other than the ones referenced and that I have indicated passages taken from those sources.

This thesis was not previously submitted in identical or similar form to any other examination board, nor was it published.



.....
Martin Kainrath

Wels, January 2018

Abstract

Dangerous situations and serious damages on electrical components caused by electric arcs during a switching process are ubiquitous. For a complete interruption of the electric circuit, the conductive electric arc has to be extinguished. In order to investigate the efficiency of an arc chute in a miniature circuit breaker, the exact arc structure and arc motion have to be analyzed. A considerable disadvantage of regular two dimensional high speed filming is the loss of depth information. Therefore, this paper proposes a method to investigate the emergence and expansion of an electric arc with a three dimensional high speed filming setup. First of all, literature research about existing three dimensional high speed filming methods followed by finding an appropriate image processing software, was done. The next step was the research for a simple calibration setup, to adjust the system for performing simplified experiments regarding to three dimensional reconstruction. To gain knowledge about the image processing software and obtain first results, known shapes were investigated. After all parameters were adjusted, the successful three dimensional reconstruction of a simple contour was discernible. In order to improve the final result, a second test series with covered simple shapes was done. The reason for covering the test objects was to increase the contrast. The aim of the final experiments was a satisfying reconstruction of a complex shape, similar to an electric arc. A successful generation of a three dimensional image by means of a branch as test object was the final outcome. An expansion in all three dimensions was clearly evident. However, electric arcs are not only dangerous in electronic devices, special cases like lightnings during a thunderstorm are mostly unpredictable. The proposed method in this work could also help to investigate atmospheric discharges, study their emergence, structure and movement.

Contents

Sworn declaration	II
Abstract	III
1 Introduction	1
2 Theory	4
2.1 Projective Geometry	4
2.2 The Pinhole Camera Model	5
2.3 Extrinsic Parameters	6
2.4 Intrinsic Parameters	6
2.5 Correspondence Problem	7
2.6 Stereo Camera Calibration	7
2.7 3D Point Reconstruction	9
2.8 Triangulation Method	9
2.9 Theory Conclusion	10
3 Scientific Question	11
4 Scientific Approach	12
5 Experimental Setup	13
5.1 Hardware	14
5.2 Software	14
5.3 Calibration Method	15
5.3.1 Calibration Pattern	15
5.3.2 Calibration Software	15
5.3.2.1 Radial Distortion	16
5.3.2.2 Tangential Distortion	17
5.3.2.3 Skew	18
5.3.3 Calibration Results	18
5.4 Data Post Processing	20
6 Experiments	25
6.1 Simple shapes	25
6.2 Covered simple shapes	25
6.3 Complex shapes	25

7	Results and Discussion	27
7.1	Simple shapes	27
7.2	Covered simple shapes	28
7.3	Complex shapes	29
8	Conclusion	35
9	Future Work	36
9.1	Different resolution	36
9.2	Reconstruction of high resolution images	36
9.3	Scaling	36
9.3.1	Reference objects	36
9.4	High speed 3D-Particle tracking	37
9.5	Atmospheric Discharges	37
9.5.1	Calibration	37
9.5.2	Synchronization	37
10	List of figures	39
11	Bibliography	41

1 Introduction

If a switch in an electric circuit is opened an electric arc occurs. In order to avoid damages and dangerous situations, electromechanic switches like miniature circuit breaker (MCB) interrupt short circuit currents in a current limiting manner. [1] Arc chutes are the core technology for electromechanic switches. The principal construction of an arc chute in an electromechanic switch is shown in Figure 1.1. After the contact separation, the arc is lengthened before the splitter plates are splitting the arc into a certain number of small series arcs in order to achieve a high arc voltage and finally extinguish it. [1]

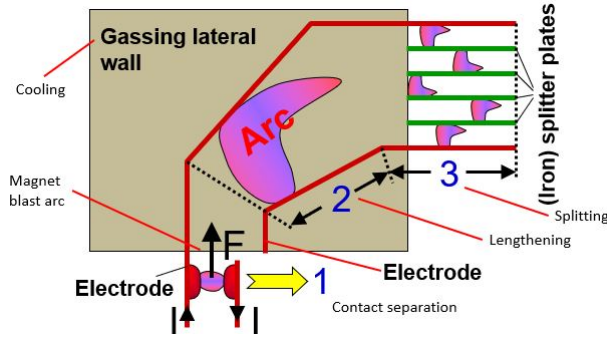


Fig. 1.1: Arc chute principles [1]

A simple equivalent circuit diagram of a basic electric circuit including a switch is shown in Figure 1.2. The source voltage $u_0(t)$ is considered to be an AC supply, $u_S(t)$ is defined as the switch voltage and $u_L(t)$ is called load voltage. R_G and L_G are the thevenin equivalent of the source. The three possible states of the circuit are: switch is closed, switch is open with an arc between the contacts or switch just open. According to Kirchhoffs laws [2], all corresponding voltages in the appropriate states are displayed in Figure 1.2 as well. Furthermore, the governing equation of the circuit is given by equation 1.1. (normal operation current neglected) [1]

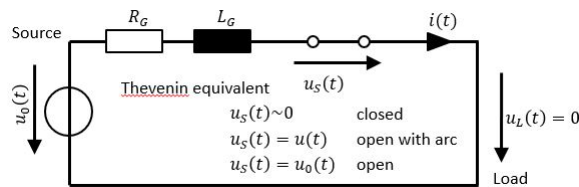


Fig. 1.2: Basic electric circuit with a switch [1]

$$u_0(t) - u_S(t) = iR_G + \frac{d_i}{dt}L_G = \hat{u}\sin(\omega t + \phi) - u_S(t) \quad (1.1)$$

To achieve the current limitation or interrupting DC Systems at all, high arc voltage arc chutes are required. Figure 1.3 and Figure 1.4 illustrate the difference of an arc extinction with and without

a counteracting switch voltage. $u_0(t)$ is defined as the AC source voltage. After the short circuit is initiated through the switch, the current increases to the maximum possible current, which is many times higher than the normal operation current (see Figure 1.3). The current limiting manner of an electromechanic switch is shown in Figure 1.4. An increasing switch voltage u_s causes a limitation of the short circuit current, immediately after the switch is opened and the short circuit is initiated. The voltage variation of the circuit (Figure 1.2 for each state (closed, open with arc, open)) is shown below the x-axis in Figure 1.4. [1]

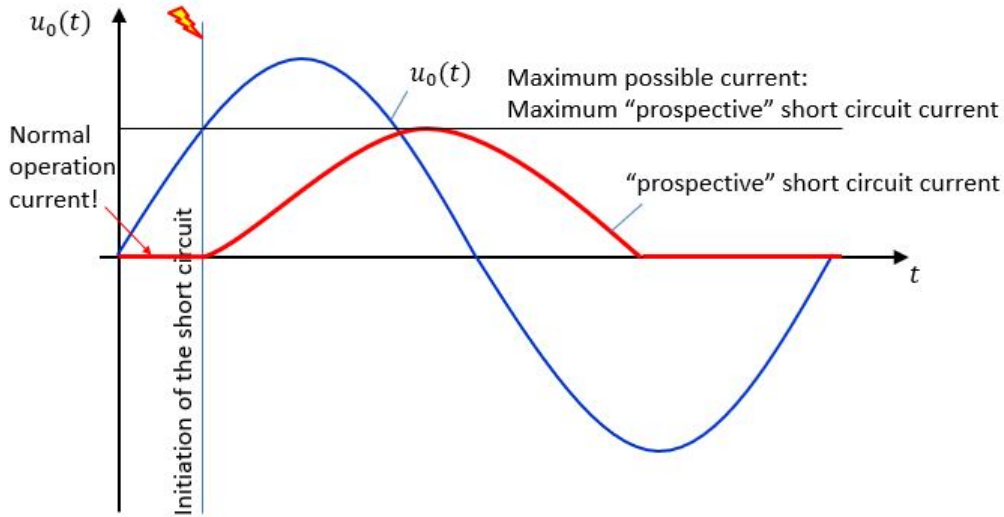


Fig. 1.3: No counteracting voltage [1]

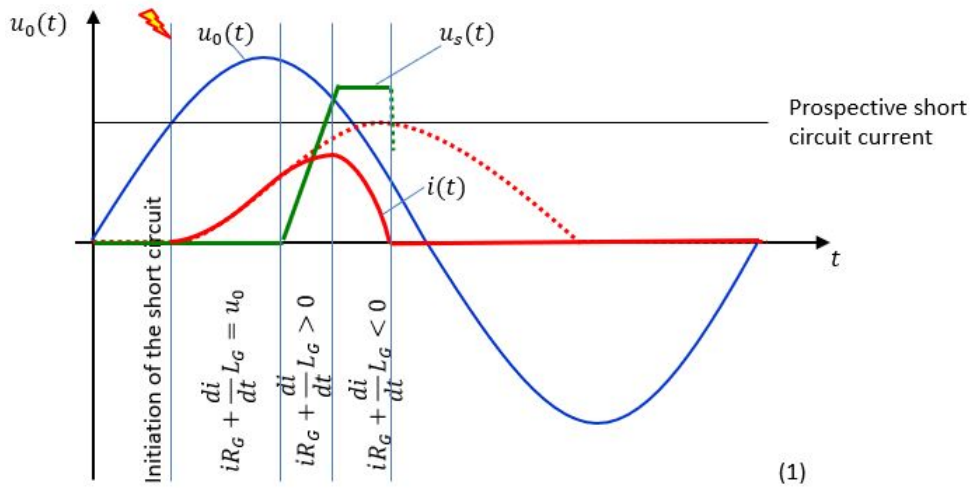


Fig. 1.4: Counteracting voltage [1]

In order to optimize arc chutes, experimental work and special diagnostic systems such as:

- high speed filming of arc motion
- pressure measurement
- temperature measurement
- gas dynamic diagnostics

- density measurement

has to be done. [1]

For almost all investigations regarding to electric arcs it is sufficient to use regular two dimensional high speed filming. Advanced studies regarding to the detailed analysis of the expansion in all possible directions requires a three dimensional image. According to Qian Wangs [3] thesis, a reconstruction of a flame using three CCD Cameras arranged around the center in an angle of 120 degrees, the aim of this work is using a similar setup to achieve a three dimensional high speed film of an electric arc.

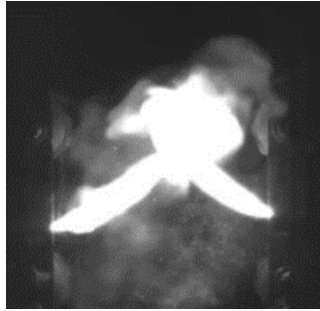


Fig. 1.5: Two dimensional image of an electric arc [4]

An image in general is the projection of a three-dimensional scene onto a two-dimensional layer, where the depth is lost. Figure 1.5 shows one image from a two dimensional high speed film of an electric arc. It is impossible to determine which one of the two plasma jets (left or right hand side) is in front or behind the other one.

The existing three-dimensional filming technology as it is known from cinemas is based on stereoscopies. Most stereoscopic methods present two offset images separately to the left and right eye of the viewer. These two-dimensional images are then combined in the brain to give the perception of three-dimensional depth. This technique is distinguished from three-dimensional displays that display an image in three full dimensions, allowing the observer to increase information about the three-dimensional objects being displayed by head and eye movements. Based on the principle of stereoscopy, three-dimensional photography also works with two-dimensional images recorded from different perspectives, but it is not the aim to create an illusion to the human eye, but rather a precise figure and measurement of the electric arc.

2 Theory

2.1 Projective Geometry

The projective geometry is used to display a three-dimensional object on a two-dimensional plane. Artists have applied this technique for hundreds of years to transfer the depth information of a real object to a sheet of paper on an easel. The transformation of a 3D Point $\mathbf{P} (X, Y, Z)$ to a plane in the Euclidean coordinate system is shown in Figure 2.1. [5]

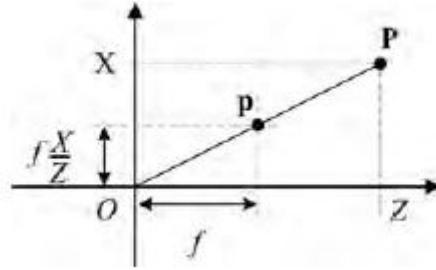


Fig. 2.1: Relationship between \mathbf{P} (real World Point) and \mathbf{p} (mapping on the projective Plane) [5]

It is assumed, that the center of the projection is at the origin $\mathbf{O} (0, 0, 0)$ and the projective plane at a distance f from the origin. If point \mathbf{p} has the coordinates (x, y) on the plane, therefore the relationship between real word coordinates and the Euclidean coordinates could be described through similar triangles:

$$x = f \frac{X}{Z}, \quad y = f \frac{Y}{Z}, \quad z = f \quad (2.1)$$

Unfortunately, these equations are nonlinear with respect to Z . The easiest way to convert them to linear equations is the addition of an extra coordinate, which means to extend the space as follows: [5]

$$\begin{bmatrix} x \\ y \end{bmatrix} \iff \begin{bmatrix} \tilde{x} \\ \tilde{y} \\ \tilde{z} \end{bmatrix} = \mathbf{P} \begin{bmatrix} X \\ Y \\ Z \\ 1 \end{bmatrix} \quad (2.2)$$

Equation 2.2 includes the Projective Matrix \mathbf{P} , which is the transformation matrix between the three-dimensional world coordinates and the image plane. \mathbf{P} is a 3×4 matrix which is a diagonal 3×3 matrix with an additional vector $[0, 0, 0]^T$ at the last column. The coordinates $\tilde{x}, \tilde{y}, \tilde{z}$ in equation 2.2 are called homogenous coordinates of a point [5].

2.2 The Pinhole Camera Model

This model is helpful to understand the mathematical relationship between real world 3D point coordinates and its projected 2D coordinates on an image plane. There are several similar models, but the pinhole camera model is the most common system. It was discovered and investigated 2500 years ago, when Euclid reported that the light projections on walls darkened rooms [6]. The model is shown in Figure 2.2, it consists of an image plane (film strip in a camera), a plane with a pinhole between the real object and the image plane (camera lens), and the real object in front of the camera.

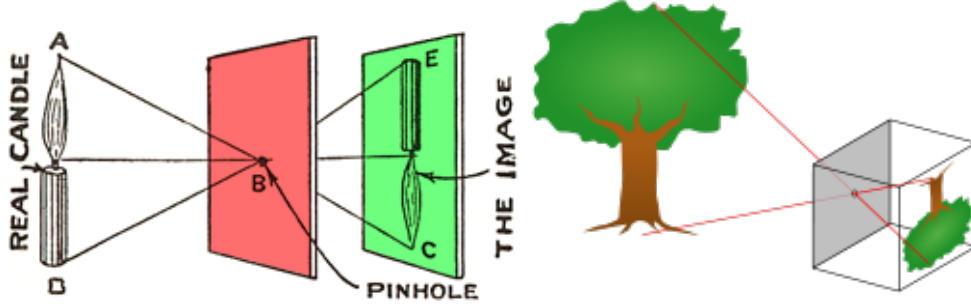


Fig. 2.2: Two examples for a Pinhole Camera Model [7], [8]

Basically, the camera and the object are defined in their own coordinate system. The internal camera coordinate system is called C, the external world coordinate system W. Figure 2.3 displays these two coordinate systems [6].

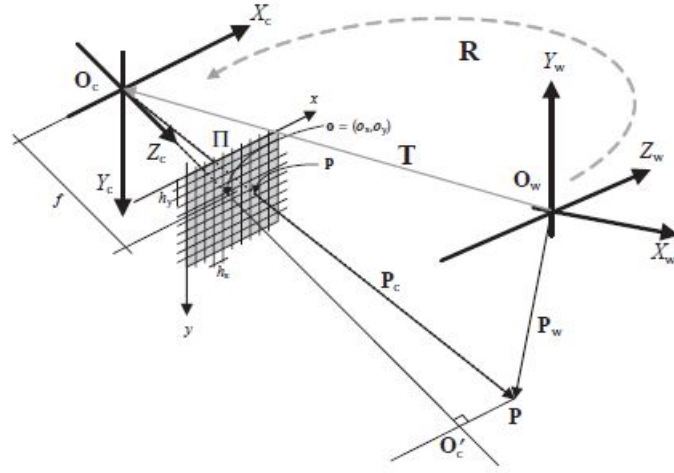


Fig. 2.3: World coordinate system (W) and camera coordinate system (C) [5]

To define the pinhole camera model completely, two sets of parameters needs to be provided [5]:

- Extrinsic Parameters
- Intrinsic Parameters

2.3 Extrinsic Parameters

The relationship between the camera coordinate frame to the world coordinate frame is called extrinsic parameters. A correct mathematical description requires a reference coordinate system, which is the camera coordinate frame in this case. An alternation of the camera frame in respect to the world frame is accomplished through a translational and rotational movement. To describe the shift of \mathbf{O}_C in respect to \mathbf{O}_W it just requires the translation vector \mathbf{T} . For the specification of a rotational movement it is necessary to implement a 3x3 matrix called \mathbf{R} (rotational matrix) [6]:

$$\mathbf{R} = \begin{bmatrix} R_{11} & R_{12} & R_{13} \\ R_{21} & R_{22} & R_{23} \\ R_{31} & R_{32} & R_{33} \end{bmatrix}, \quad \mathbf{T} = \mathbf{O}_W - \mathbf{O}_C = \begin{bmatrix} T_1 \\ T_2 \\ T_3 \end{bmatrix} \quad (2.3)$$

In example, for a given Point P in world coordinates, the transformation to the camera coordinate frame would be as follows [6]:

$$P_C = \mathbf{R}(P_W - T) \quad (2.4)$$

2.4 Intrinsic Parameters

These parameters can be separated into three categories [6]:

1. The parameters used for the projective transformation: for the pinhole camera model it is just the focal length f .
2. The parameters for the description of the coherence between the internal camera frame and the image plane frame. The origin of the image coordinate frame is for example in one corner or in the center of the image. In Figure 2.3 it is assumed that the principal point of the image frame is in the center of the image plane, given by o_x and o_y . Finally, the relationship between the image coordinates and the camera coordinates can be calculated as follows [6]:

$$x = (x_u - o_x)h_x \quad (2.5)$$

$$y = (y_u - o_y)h_y \quad (2.6)$$

whereas h_x, h_y are physical dimensions of the pixels and usually given in micrometers, x_u, y_u are the image coordinates.

3. Characterization of tangential and radial lens distortions. These parameters are nonlinear and based on geometric equipment inside the cameras. In most of the cases it is decent to neglect them [5].

Based on this knowledge, it is possible to write the result in a mathematical way with the Intrinsic matrix A:

$$\mathbf{X} = \mathbf{A}\mathbf{p} \quad (2.7)$$

$$\mathbf{R} = \begin{bmatrix} x_u \\ y_u \\ 1 \end{bmatrix}, \mathbf{T} = \mathbf{O}_W - \mathbf{O}_C = \begin{bmatrix} \alpha_u & \gamma & o_x \\ 0 & \alpha_v & o_y \\ 0 & 0 & 1 \end{bmatrix} \begin{bmatrix} x \\ y \\ 1 \end{bmatrix} \quad (2.8)$$

\mathbf{A} is a 3x3 matrix and contains α_u and α_v which are the focal lengths for the pixel axis (u, v) respectively, and γ skew parameters between the pixel axis. $X = [X, 1]$ and $p = [p, 1]$ are the homogenous coordinates [6].

The projective matrix from equation 2.2 can be written with the usage of the extrinsic- and intrinsic parameters:

$$\mathbf{P} = \mathbf{A} [\mathbf{R} \quad \mathbf{T}] \quad (2.9)$$

Equation 2.2, 2.8 and 2.9 applied on each other resulting in the complete projection equation [6].

$$k \begin{bmatrix} x & y & 1 \end{bmatrix} = \begin{bmatrix} \alpha_u & \gamma & o_x \\ 0 & \alpha_v & o_y \\ 0 & 0 & 1 \end{bmatrix} [\mathbf{R} \quad \mathbf{T}] \begin{bmatrix} X & Y & Z & 1 \end{bmatrix} \quad (2.10)$$

Extrinsic and intrinsic parameters are provided by stereo camera calibration, k is a scale factor [6].

2.5 Correspondence Problem

After determining parameters for the system, the next step is to find corresponding points between the images. Epipolar geometry is helpful to constrain the number of appropriate points and minimizes computation time. Figure 2.4 represents the structure of epipolar geometry [6].

C_r, C_l are the optical centers of both cameras and together with M they are generating the epipolar plane π . The baseline is defined through the connection of both camera centers. The intersection point of the baseline and the image plane is defined as epipole (e_r, e_l) . The intersection lines of the image planes with the epipolar plane are called epipolar lines. As shown in Figure 2.4, the depiction of point M on the left image plane (m_L) must be on an epipolar line on the right image plane (m_r) . [3]

2.6 Stereo Camera Calibration

For a satisfying result of three-dimensional photography, it is necessary to calibrate both cameras. After a successful calibration, the intrinsic parameters of the camera and extrinsic parameters of the setup may be derived. There are several types of calibration as standard, photometric, or self-calibration. Standard calibration is the easiest and most common way and was proposed by Zhang. [9] It works with a simple pattern (i.e. chessboard) obtained from a laser printer and mounted on a rigid surface. At least two pictures with different orientations of the pattern are needed to compute the

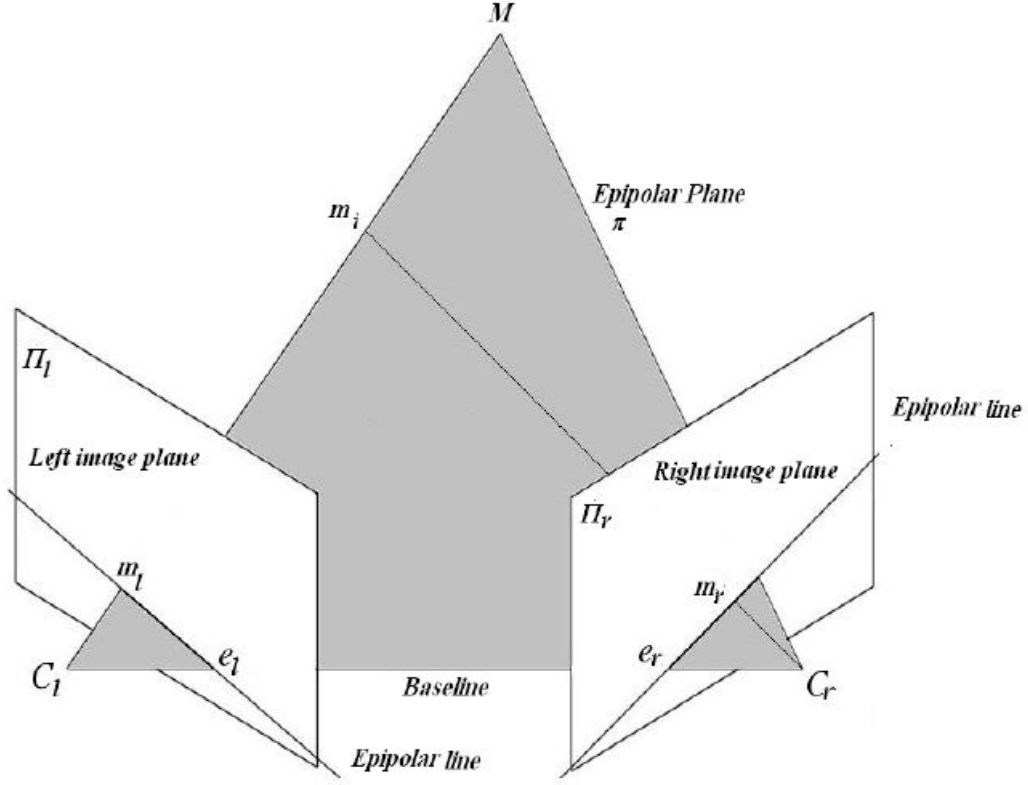


Fig. 2.4: Epipolar geometry [6]

required parameters. If a chessboard is used, it is important to know the size of the black squares. The edges of these squares are the objects, the feature extracting algorithm is looking for. However, to calculate the extrinsic and intrinsic parameters, equations 2.3, 2.5 and 2.6 are combined and providing the following result [6]:

$$x - o_x = -h_x \frac{R_{11}X^w + R_{12}Y^w + R_{13}Z^w + t_1}{R_{13}X^w + R_{32}Y^w + R_{33}Z^w + t_3} \quad (2.11)$$

$$y - o_y = -h_y \frac{R_{21}X^w + R_{22}Y^w + R_{23}Z^w + t_1}{R_{13}X^w + R_{32}Y^w + R_{33}Z^w + t_3} \quad (2.12)$$

To solve equation 2.11 and 2.12, it is required to use the known points from the calibration pictures. For the determination of the projective matrix, a second algorithm is used. Equations 2.2 and 2.9 together with the known extrinsic and intrinsic parameter are leading to the following relations [6]:

$$x = \frac{x_u}{z_u} = \frac{P_{11}X^w + P_{12}Y^w + P_{13}Z^w + P_{14}}{P_{13}X^w + P_{32}Y^w + P_{33}Z^w + P_{34}} \quad (2.13)$$

$$y = \frac{y_u}{z_u} = \frac{P_{21}X^w + P_{22}Y^w + P_{23}Z^w + P_{24}}{P_{13}X^w + P_{32}Y^w + P_{33}Z^w + P_{34}} \quad (2.14)$$

x_u, y_u, z_u are representing the coordinates of image points expressed in camera coordinates. Equations 2.13 and 2.14 contain eleven unknown variables, which can be determined through eleven or

more known points from the image of the calibration pattern. [6] The computation and solution of these four equations 2.11, 2.12, 2.13 and 2.14 is usually done by appropriate software (i.e. MATLAB).

2.7 3D Point Reconstruction

The purpose of three-dimensional point reconstruction is to acquire certain information of the three-dimensional structure displayed on the two-dimensional image. The accuracy of the reconstruction depends on the quality of the result of the camera calibration. In case of inaccurate or missing calibration data, it is not possible to obtain absolute Euclidean coordinates of the reconstructed point. A precise description of the nonlinear dependency between the accuracy of the calibration parameters and the reconstruction process based on available disparities extracted from stereo-pair images was presented by Grimson. [10] For this research project, it is sufficient to know the three different characteristic cases regarding to the calibration data [5].

1. If extrinsic and intrinsic parameters are available, a complete three-dimensional reconstruction in Euclidean coordinates is possible through triangulation.
2. For the availability of only intrinsic parameters, the reconstruction can be done up to a certain scaling factor.
3. If neither extrinsic nor intrinsic parameters are available, reconstruction can be done up to a certain projective transformation.

2.8 Triangulation Method

The triangulation method is an approach to determine the coordinates of a certain point in three-dimensional space as shown in Figure 2.5 [5].

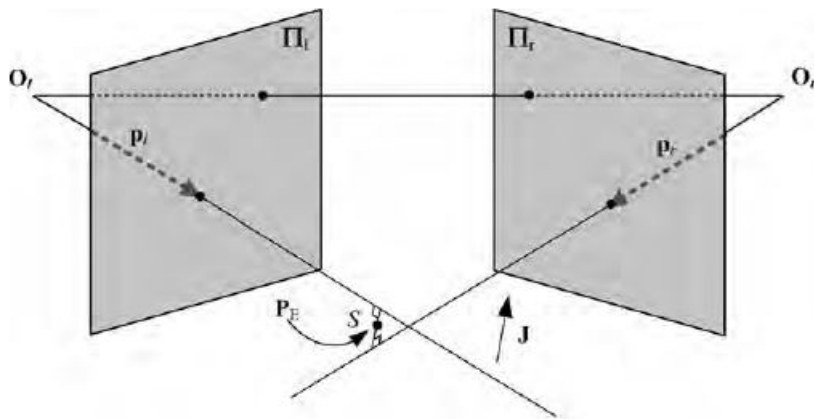


Fig. 2.5: Triangulation method [5]

After a successful camera calibration and with known corresponding image plane points P_L and P_R it should be possible to find an intersection point between the two beams defined with the starting points O_L and O_R and the image plane points P_L and P_R . In practice, these two beams will never

intersect in a certain point, hence it is necessary to find an approximation intersection point, called P_E . A line which is orthogonal to both beams, and defines the minimal distance between them. P_E is in the middle of the line, in simultaneous distance to both beams. MATLAB is able to compute and display all these points in a three-dimensional plot and finally an initially three-dimensional scene, displayed onto two images became a three-dimensional structure again [5].

2.9 Theory Conclusion

The 3D reconstruction method described in chapter 2 is probably the only useful method in terms of high speed applications. One way for a better reconstruction result would be a movement of the camera while taking a sequence of images, called Structure from Motion (SfM). Unfortunately, a camera movement in electric arc investigation is clearly not possible, because arcs in switching devices are very fast, unstable and only visible for a few milliseconds. During the camera movement in a SfM reconstruction, the test object (arc) should not move at all. Another way would be a test setup including more than two cameras, for more images of the same scene taken from different point of views. Regarding to the fast expansion and direction change of arcs, a complete synchronization of the system would be required.

3 Scientific Question

Based on the approach in section 2.5, 2.6, 2.7 and 2.8, the three dimensional reconstruction out of two captured images should be investigated. Deliberations about the experimental setup in general and all the required components for such a project have to be done. The right positioning of the cameras during the experiments in this work has to be considered. Especially, the influence to the final result in terms of angle variation between the cameras should be investigated. Furthermore, simple, known test objects (i.e. a cube, a sphere or a cuboid) can be helpful for the first attempts to obtain simplified reconstruction results. The compatibility of the system for a combination of one black and white and or a coloured image has to be verified, because the setup should be able to work with any combination of high speed cameras, either black and white or colored captured images.

4 Scientific Approach

The aim of this work is to identify an appropriate setup to generate a digital three dimensional model of an electric arc out of a real scene recorded in high speed. After deliberations about the construction of the system itself were done, some simple experiments should be performed to proof the functionality of the setup. These experiments should also help to investigate the required calibration of the system and find a proper method to calibrate easily. Another important objective in this work is the research for a appropriate image processing and calibration software. Finally, a reconstruction of the recorded test object to a three dimensional image and an appropriate visualization should be done.

5 Experimental Setup

For a satisfying three dimensional reconstruction result of an electric arc, a well-working setup is needed. Basic requirement for recording an fast process with a time period of a few milliseconds is a CCD high speed camera. The reconstruction procedure requires two or more images of the same scene, which is easy to implement for a stationary object. Arcs are very unstable and in some cases only visible for a short period of time. Therefore, the two images has to be captured in the exact same moment. There are two possible ways to solve this problem:

- Two fully synchronized CCD Cameras
- Mount a stereo adapter in front of the camera

If two cameras are available, the synchronization could be done via external sync input signals or one camera generates the sync output (master) for the sync input of the second camera (slave). To save costs, a stereo adapter system for a CCD camera was used for experimental work by Mahmoud Abdul-Latif Assad [6]. In comparison to Assad, the two camera setup should be preferred for this project. However, the next step to complete the whole setup would be appropriate software (i.e. MATLAB, LABVIEW,...) and hardware for data processing and visualization. Figure 5.1 shows a simple sketch of the possible final experimental setup.

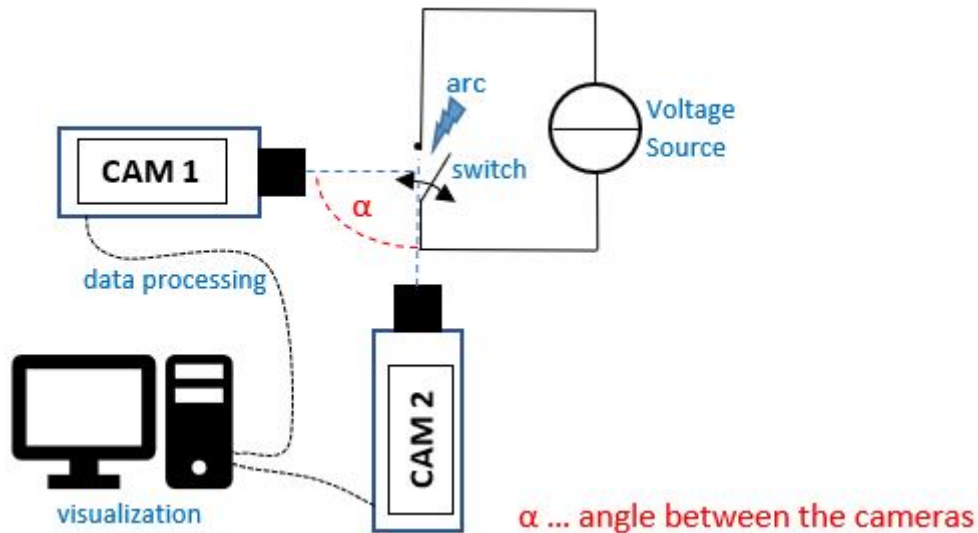


Fig. 5.1: Possible final setup

For the first experiments, a simple setup including two digital cameras and basic test objects could be used to understand each step of the reconstruction process done by the software. Nevertheless, either simple or complete system, it has to be calibrated at the beginning. The calibration process

could be done by taking pictures of known contours, for instance a method proposed by Zhang [9] using a chessboard with known square size, take pictures and compute the required parameters afterwards.

As mentioned before, two simple digital cameras were used in the testing phase to get used to the three-dimensional reconstruction process. Mounted on tripods and arranged in the opposite of a white background. The tripods were fixed on a heavy table in the laboratory to suppress vibrations during the photo sessions. The internal camera settings were set equal for both cameras. Due to the fact, that the resolution of images taken with high speed cameras decreases for a higher frame rate, the resolution in the camera settings was set to the minimum of 640x480 pixels. For the investigation of the reconstruction result depending on resolution, images with a higher resolution were taken as well. Furthermore, the quality of the outcome is heavily dependent on the angle α between the two camera lenses. To investigate the influence of different positions of view onto the generating of the result, the camera angle α was varied.

5.1 Hardware

As already mentioned, the CCD cameras were replaced with simple digital cameras (see Figure 5.2) for the experiments. Some technical facts about the cameras and other used equipment are listed below.

- Polaroid iS048 Digital Camera¹
 - > 16 Megapixels
 - > CMOS Sensor
 - > Image Resolution: VGA(640x480) up to 16M (4608x3456)
 - > Lens: f=8.15mm F3.0
 - > USB 2.0
- Flexible tripods
- Different test objects (cubical, cylindrical, ...)



Fig. 5.2: Digital camera Polaroid is048

5.2 Software

After a quick review of possible image processing software tools, MATLAB 2017a was found to suit the requirements best. The simple handling and lots of available image processing functions for the purpose

¹<http://www.polaroid.com/products/polaroid-is048>

of this project were the reasons to choose MATLAB. Furthermore, the stereo camera calibration app provided by MATLAB made the calibration process easier and it was not necessary to write and execute the whole calibration code manually.

5.3 Calibration Method

5.3.1 Calibration Pattern

The best pattern for a successful calibration is a regular chessboard, because it has easy detectable edges and corners. The calibration pattern for this series of tests was a chessboard with a square size of 28.8mm x 28.8mm. Printed out on from a regular printer and stuck on a cardboard to create a flat surface. Figure 5.3 shows the experimental setup, including the calibration pattern.



Fig. 5.3: Test setup during calibration process with pattern

5.3.2 Calibration Software

Before the three-dimensional reconstruction algorithm can be applied to the captured images, the system needs to be calibrated. For this project, the Stereo Camera Calibrator App in the MATLAB Computer Vision Toolbox was used. As already mentioned in section 2.6 at least two images are required to get calibration data, but MATLAB strongly recommends between 10 and 20 images for a satisfying result. The user interface of the calibration app is shown in Figure 5.4.

After about 15 pictures from different pattern orientations were taken, they had to be imported into the app. It is important to choose the angle between one camera and the pattern not too narrow, because otherwise MATLAB is not able to detect the corners correctly and will reject the image pair. As shown in Figure 5.5, the angle β between the pattern and the camera lens should always be wide enough to avoid errors during the calibration process.

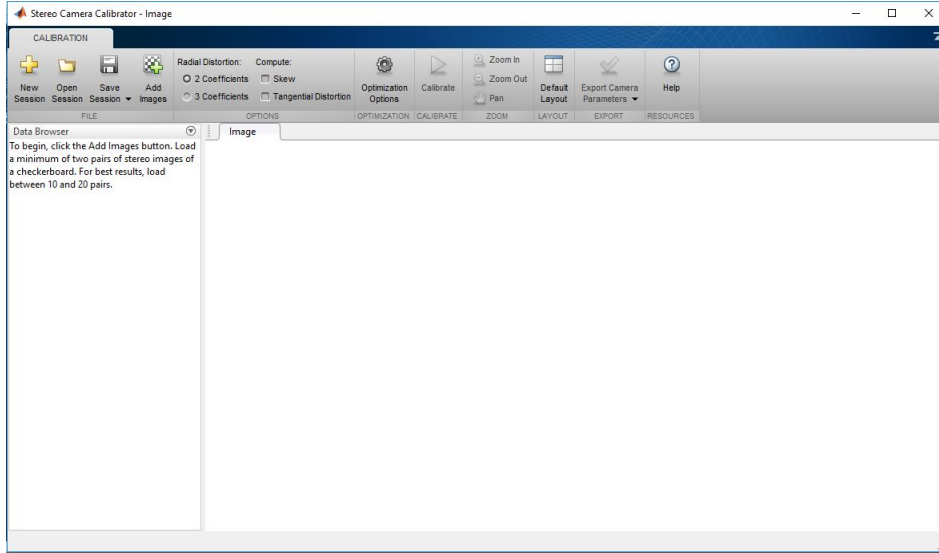


Fig. 5.4: MATLAB Stereo Camera Calibration App

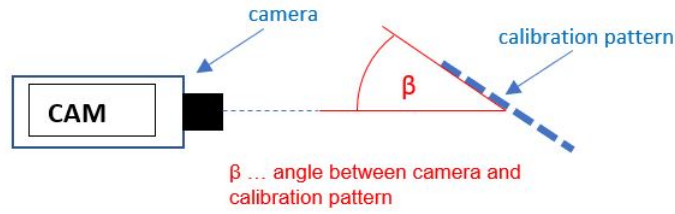


Fig. 5.5: Camera and calibration pattern

It is necessary to enter the size of the squares from the chessboard in world units, to find a mapping between real world units and image pixels. The checkerboard calibration pattern is then detected automatically in every image pair by the app. MATLAB shows all the images and detected edges in a preview on the left hand side. To check the accuracy of the checkerboard detector, every image pair can be opened, zoomed in and probably removed, if the corner detection is incorrect or not good enough. Figure 5.6 displays the calibration app after importing calibration images.

Before starting the calibration process, the number of radial distortion coefficients can be specified in the menu bar. If necessary the tangential distortion and skew can be computed as well.

5.3.2.1 Radial Distortion

Radial distortion is the phenomena, that occurs when light beams bend more near the edges of a lens than at its optical center. For smaller lenses, the distortion increases. The radial distortion coefficients are representing various types of distortion shown in Figure 5.7. The distorted points are denoted as $(x_{distorted}, y_{distorted})$ and can be derived from equation 5.1 and 5.2 [11]

$$x_{distorted} = x(1 + k_1r^2 + k_2r^4 + k_3r^6) \quad (5.1)$$

$$y_{distorted} = y(1 + k_1r^2 + k_2r^4 + k_3r^6) \quad (5.2)$$

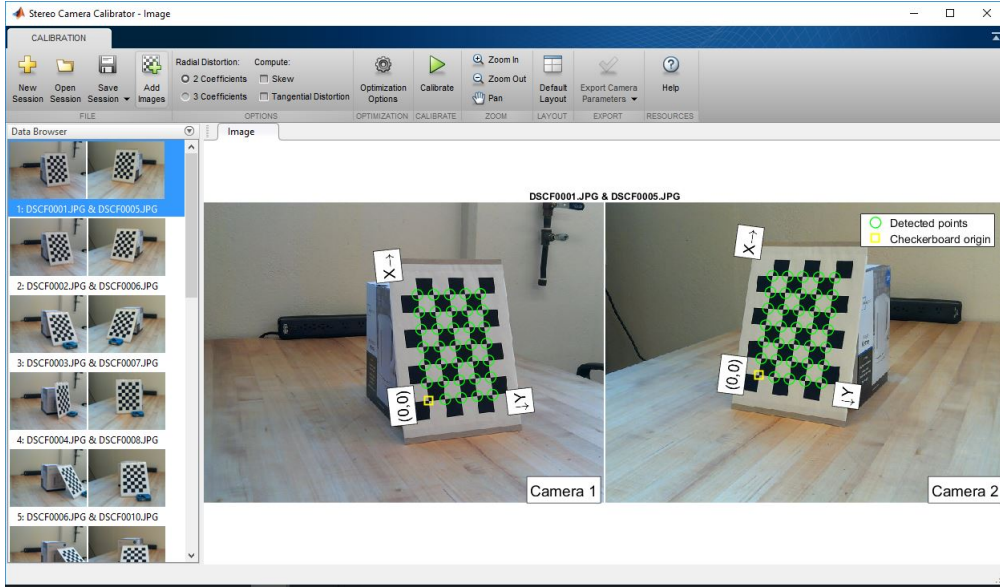


Fig. 5.6: Calibration App with imported pattern images

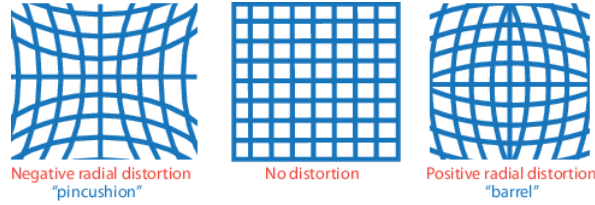


Fig. 5.7: Different types of radial distortion [11]

- x, y — Undistorted pixel locations. x and y are in image coordinates. Image coordinates are optical center translated pixel coordinates and dividing by the focal length in pixels. x and y are dimensionless values.
- k_1, k_2 and k_3 — Radial distortion coefficients
- $r^2 = x^2 + y^2$

Commonly, two coefficients are sufficient, but for severe distortion three coefficients are necessary. [11]

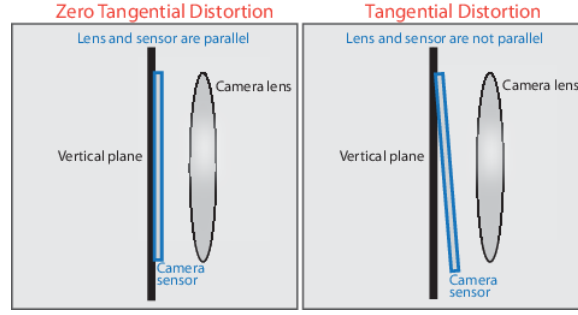
5.3.2.2 Tangential Distortion

Tangential distortion occurs when the camera internal image plane and lens are not parallel. Figure 5.8 sketches the image plane and the lens of a camera [11]:

$$x_{distorted} = x + [2p_1xy + p_2(r_2 + 2x_2)] \quad (5.3)$$

$$y_{distorted} = y + [p_1(r_2 + 2y_2) + 2p_2xy] \quad (5.4)$$

- x, y — Undistorted pixel locations. x and y are image coordinates. Image coordinates are

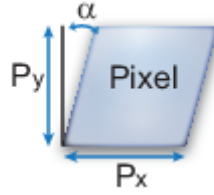
**Fig. 5.8:** Tangential distortion [11]

optical center translated pixel coordinates and dividing by the focal length in pixels. x and y are dimensionless values

- p_1 and p_2 — Tangential distortion coefficients
- $r_2 = x_2 + y_2$

5.3.2.3 Skew

The skew factor is part of the Intrinsic Parameters and is non-zero, if the image axes are not perpendicular. The definition of the skew factor is shown in Figure 5.9 [11]:

**Fig. 5.9:** Skew factor [11]

$$s = f_y \tan \alpha \quad (5.5)$$

$$f_x = \frac{F}{p_x} \quad (5.6)$$

$$f_y = \frac{F}{p_y} \quad (5.7)$$

- (p_x, p_y) — Pixel size in world units.
- (f_x, f_y) — Focal length in pixels.
- F — Focal length in world units.

5.3.3 Calibration Results

Right after all requested settings are done, the computation of the calibration data can be started. Figure 5.10 shows the user interface after the first computation of the parameters.

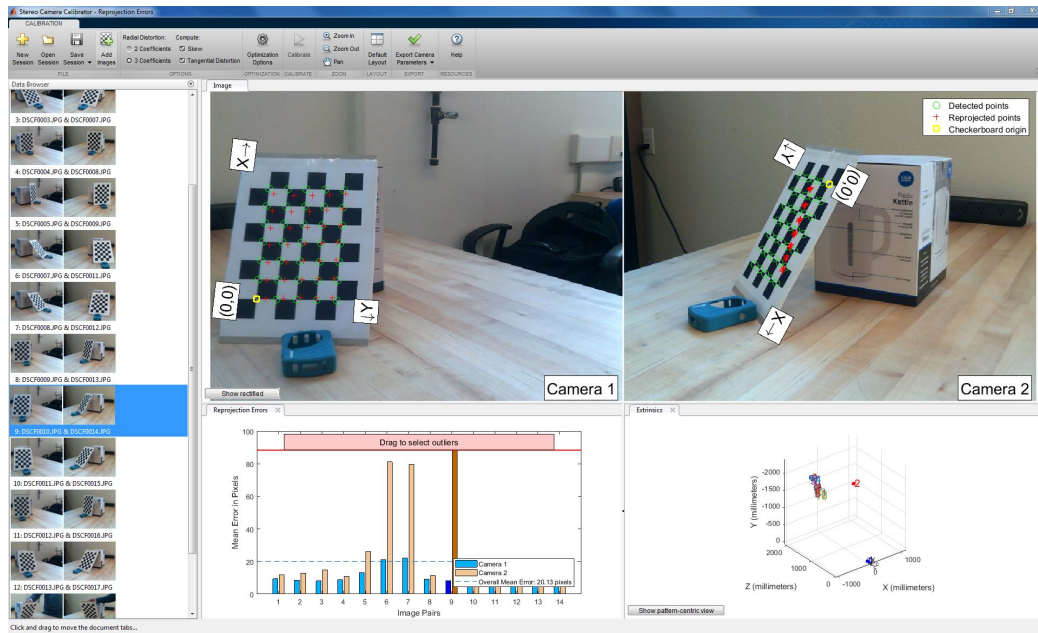


Fig. 5.10: Calibration Results after first computation

Once calibration is done, the results can be evaluated by inspecting the used images for reprojection errors. Reprojection errors are a global measurement of calibration errors and are the difference between detected points in the image and reprojected points back onto the image. For the reprojection, the actual calculated camera parameters are used already. In this case, image 6,7 and 9 in Figure 5.10 are indicating a high error and therefore they are not included for further computations. The extrinsic parameters are displayed in the bottom right corner in Figure 5.10 as a reconstruction of the real scene in Figure 5.3. Obviously, the reconstructed calibration scene is wrong because it is based on the computation with flawed images. The final calibration result after these images were removed is shown in Figure 5.11.

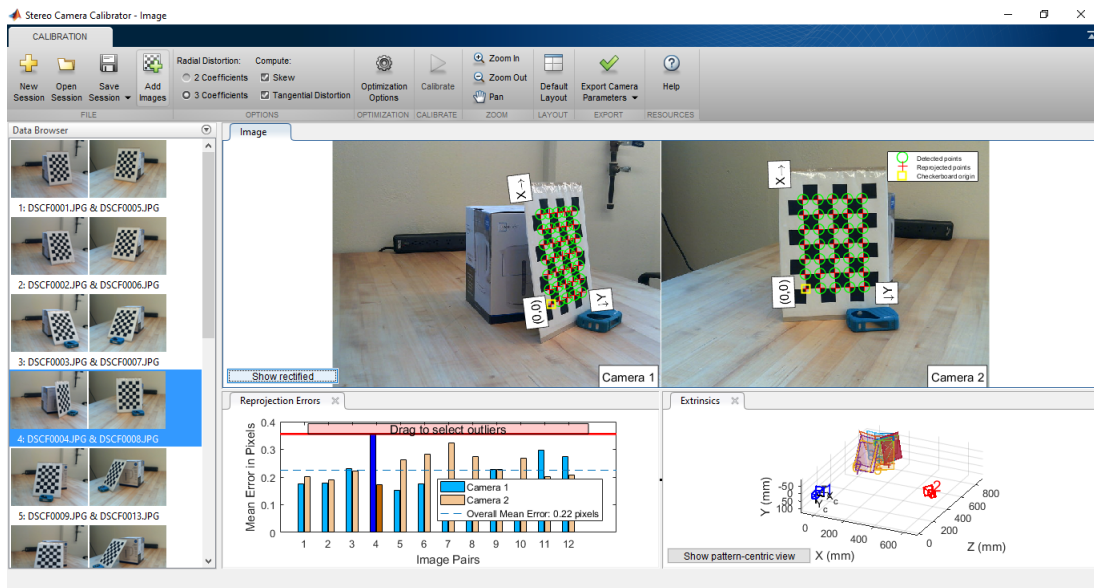
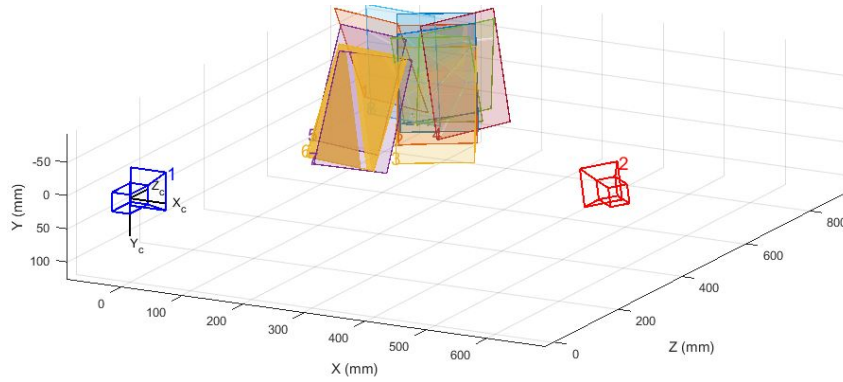


Fig. 5.11: Calibration Results final computation and a certain tolerance of accuracy

Finally, the determined calibration data can be exported to a MATLAB scrip file for further us-



(a) Real scene



(b) Reconstructed scene

Fig. 5.12: Comparison between real and reconstructed scene based on calibration data

age. Figure 5.12 illustrates the comparison of the real calibration scene to the calculated scene by MATLAB. The different coloured rectangles in Figure 5.12b are representing all pattern orientations in the captured images for the calibration. It is important, that the cameras are remaining in the same position while taking images for the calibration process and for taking images of actual objects which are going to be investigated as well. If there is a movement of one camera, the system has to be recalibrated again. In general, it is recommended to recalibrate the system at the beginning of every series of tests [12].

5.4 Data Post Processing

According to section 2.5 the analysis of two images to find corresponding points and their location in real world coordinates is done by a series of computations through MATLAB. After two images were imported from the storage to the workspace, the first step is the correction of lens distortion. This is very important, because the final result could be effected by distortions which leads to an inaccurate reconstruction. For a successful removal of lens distortion, MATLAB used the determined camera parameters from the previous calibration process. The next step is matching a sparse set of points between the two experimental images. MATLAB is able to find corresponding points of

two images in a few different ways. For this project corner detection in the first image followed by similar point tracking in the second image was used. Alternatively SURF (Speeded-Up Robust Features) features or MSER (Maximally Stable Extremal Regions) features could be detected as well. The MATLAB function "detectMinEigenFeatures" uses the minimum eigenvalue algorithm by Shi and Tomasi to detect corners in a grayscale input image and returns their x and y coordinates in a matrix. Therefore it does not matter if the input image is coloured or grayscale, "detectMinEigenFeatures" needs a grayscale image anyway. The function "rgb2gray" converts the coloured image to grayscale. Using the Argument "MinQuality" is a possibility to adjust the number of detected corners and finally for the reconstruction process. Figure 5.13 shows the detected corners in image taken by the left camera. [12]

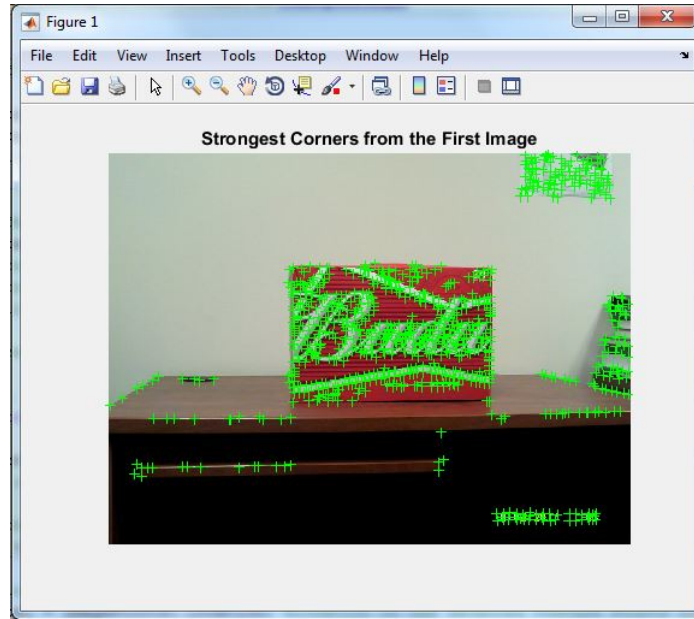


Fig. 5.13: Detected cornes using the minimum eigenvalue algorithm by Shi and Tomasi

As mentioned earlier, point tracking has to be executed next. Therefore, MATLAB provides the function "vision.PointTracker", which tracks points using the Kanade-Lucas-Tomasi (KLT) algorithm. The tracked points between both images are displayed in Figure 5.14. There are three different methods to display two images in MATLAB. The MATLAB function "showMatchedFeatures" provides "falsecolor", "blend" and "montage". "falsecolor" overlays the images by creating a composite red-cyan image showing image 1 as red and image 2 as cyan (i.e. Figure 5.15). "blend" overlays image 1 and image 2 using alpha blending and "montage" places image 1 and image 2 next to each other in the same image (i.e. Figure 5.14). [12]

For the example in Figure 5.14 the tracking procedure was quite accurate, there are just a few outliers in the background on the wall. At this point it is necessary to calculate the Essential Matrix and remove outliers. Matlab is using the "estimateEssentialMatrix" Function. To execute the computation of the Matrix, the camera parameters and the tracked points are required. Figure 5.15 shows the matched features and Epipolar inliers. [12]

As mentioned in section 2.3 the reference coordinate system is the internal coordinate system of camera 1 for this project. Based on the Essential Matrix, it is possible to compute the orientation and location of one camera relative to the other one. To calculate these parameters MATLAB provides a

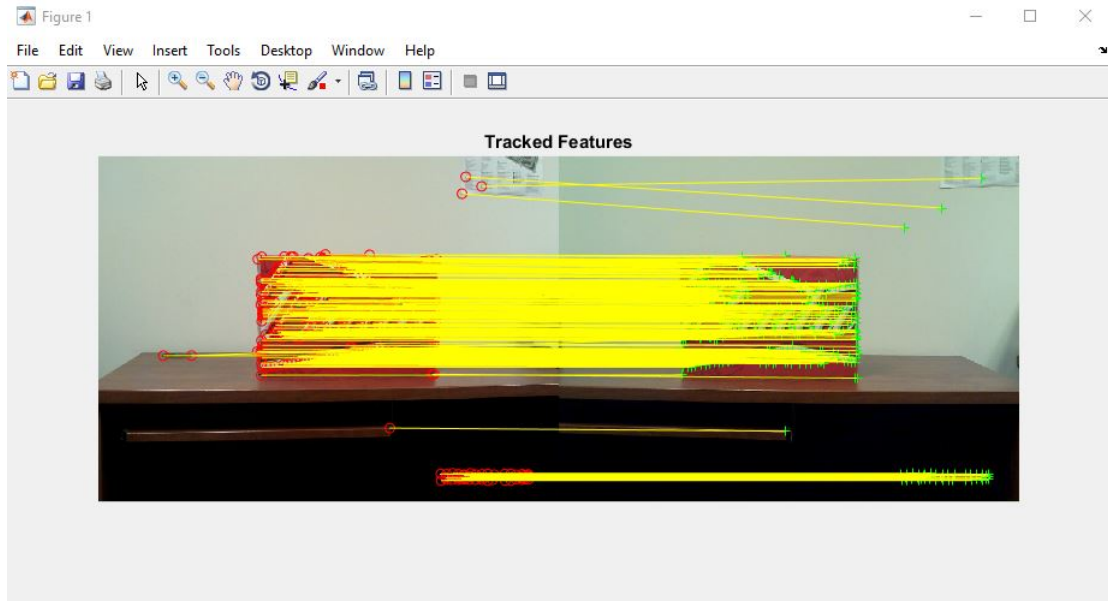


Fig. 5.14: Tracked points by the KLT algorithm in a 'montage' plot

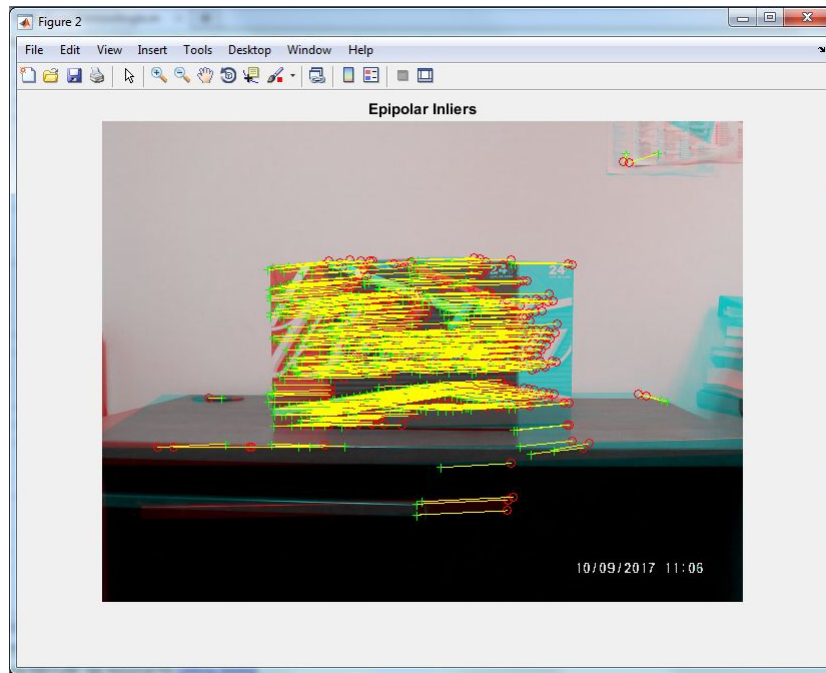


Fig. 5.15: Epipolar inliers

function called "relativeCameraPose" which returns the orientation and location of the second camera which is rotated and translated relative to the origin of the world coordinate system. The function "cameraMatrix" provides the projection matrices of both cameras for the final triangulation process. As an input, these functions need the camera parameters obtained from the calibration, the rotational matrix and the translation vector. For camera 1, the rotational matrix is given as the identity matrix and the translation vector is given as $(0,0,0)^T$, because the internal coordinate system of camera 1 is the reference system for the computation and its translation and rotation relative to the world coordinate system is zero. The triangulation function itself returns the three dimensional locations of the computed points in real world coordinates as a $m \times 3$ matrix. As input arguments both camera

projection matrices and the matched points from the tracker are required. [12] After finishing the computation, the result of the triangulation provides the needed points for the three dimensional structure. Unfortunately, during the simulation occurred some computational errors, shown in Figure 5.16

-0.8152	-1.6076	13.4670			
-0.6634	-0.4975	11.0231			
-0.8312	1.2868	13.9703			
-0.8224	0.5890	12.9870			
-0.8010	2.0980	-15.2890	2.6889	2.1208	8.6905
-0.7822	-0.0540	10.9870	1.9858	1.8014	6.4113
-0.7769	-1.3619	13.0035	2.1645	2.1347	6.9929
-0.4413	0.0897	7.5970	2.6580	1.5280	125.9830
-0.4811	1.0043	8.2454	2.8298	0.2501	9.1522
-0.3680	1.6098	6.3859	2.5947	0.7241	8.3577
-0.5267	2.2945	9.2765	2.5780	0.7466	8.3167
-0.6545	-2.4604	11.4564	2.5456	0.8477	8.2219
			2.7542	1.7018	8.8758
			2.7112	1.8460	8.7225

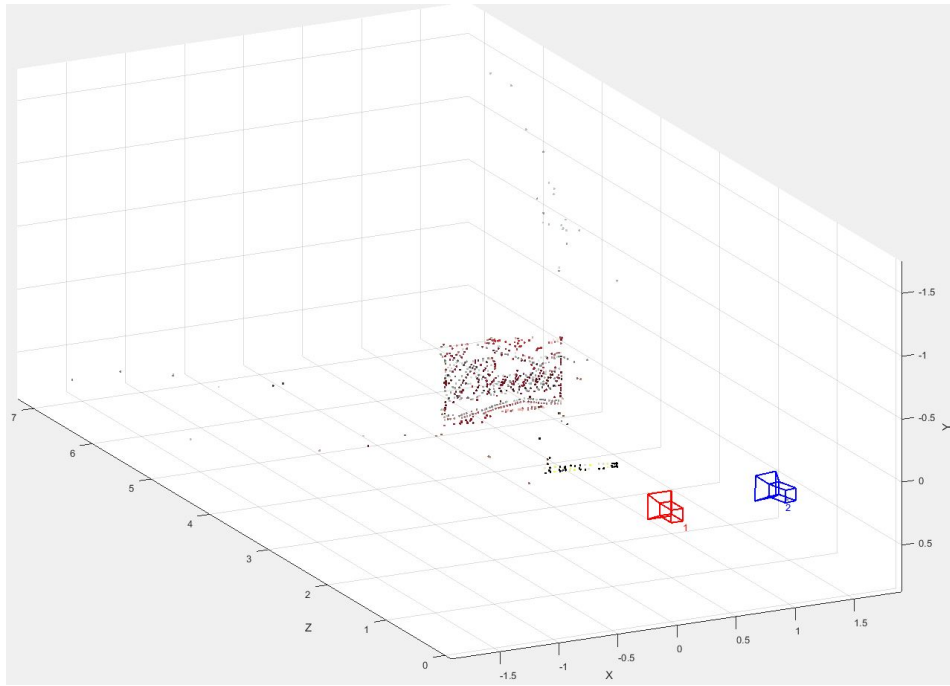
(a) negative z coordinate

(b) extraordinary high z value

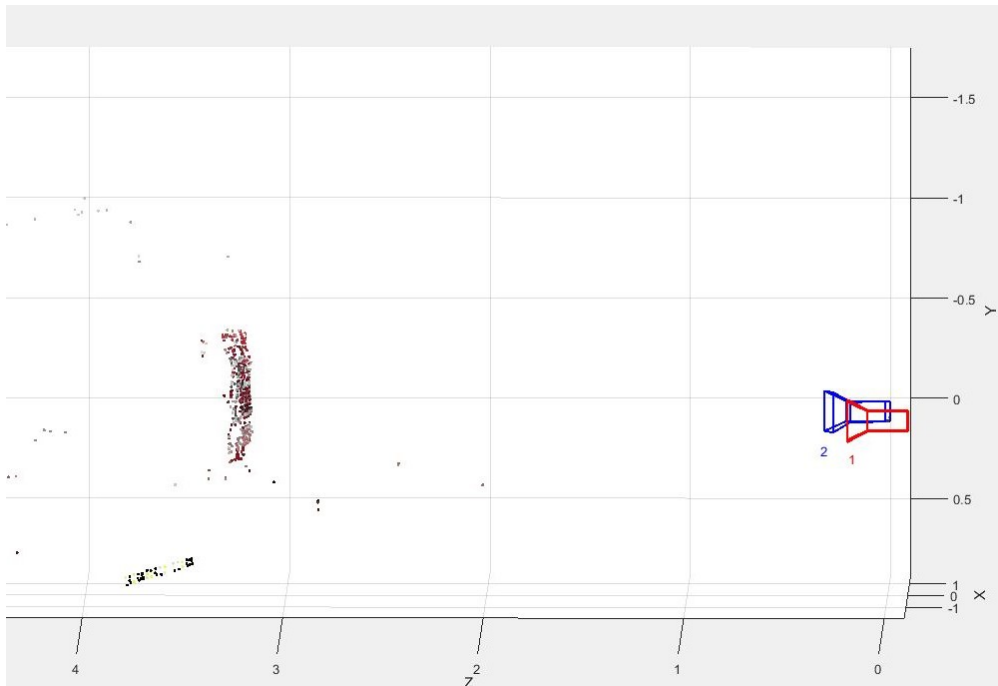
Fig. 5.16: Computation errors after triangulation

In case of figure 5.16a the z coordinate is negative. The z axis of the world coordinate system (reference coordinate system) has its origin in the internal coordinate system of camera 1. A negative z coordinate would stand for a reconstructed point behind the camera, which is clearly impossible. Another error case is shown in Figure 5.16b. The range of z coordinates for these example points is between 6.41 and 9.15, so a value of 125.98 is obviously an outlier. For a satisfying reconstruction result both errors have to be removed. To solve this problem, a point filter in form of two for loops scanning the matrix for negative values or outliers was used. A display of the matrix in the MATLAB command window is helpful to evaluate the upper and lower limit for outliers. One way to print the final results is a three dimensional point cloud plot. Using the MATLAB function "pointCloud" with the point matrix and alternatively the color as input arguments creates the required point cloud. Additionally to the three dimensional points, it is possible to show both cameras in the same plot as well. MATLAB provides the "plotCamera" function for this case, with a few input arguments for detailed representation. Figure 5.17 illustrates the final result after using all the earlier mentioned functions.

The reconstructed shape is a appropriate reproduction of the real object, up to a certain scale factor. A possible way to determine the scale factor and set the right axis scale could be to fit a known contour into the final result and measure the length of it. (see chapter 9)



(a) Front view



(b) Side view

Fig. 5.17: Three dimensional reconstruction result

6 Experiments

Based on the approach in chapter 5, some experimental setups may be established to obtain practical results. In order to save costs and start the tests in a simplified way, the following experiments were done:

- capturing stereo images of known simple shapes
- capturing stereo images of covered simple shapes for more realistic circumstances
- capturing stereo images of complex shapes to simulate an image of a high speed record of an electric arc

6.1 Simple shapes

The known dimensions of a simple shape was the reason for using them for the first test. It is easier to check the accuracy of the final result regarding to measurement and scaling errors by using simple structures as test objects. In order to review the accuracy of the contour detection by the image processing software, straight edges are helpful to show deviations between the real object and the generated digital three dimensional image. A detailed adjustment of important parameters during the reconstruction process in MATLAB is easier to realize with simple testing objects as well. Therefore, the whole reconstruction algorithm in MATLAB should be optimized before taking pictures of complex shapes.

6.2 Covered simple shapes

In order to increase the contrast between the test object and the environment, the simple shape has to be covered in one color. In the first experiment, described in section 6.1, the test objects could just be simple cardboard packaging materials. This method could reduce the outcome of the reconstruction to the outlines of the photographed objects and may help to display the transition from the the test object to the environment. Applied to an electric arc from the brightness of the plasma jet to the darkness of the ambient air.

6.3 Complex shapes

After a variety of tested simple shapes and an adjusted setup, complex shapes with a similar structure like a electric arcs should be the test objects for the last experiments. The aim of these experiments

is to find a complex shape, capture a few images and determine the direction of the expansion in all three dimensions. In order to keep it simple and minimize the reconstruction effort, the simplified setup is used again. If the reconstruction is successful, the procedure may be applied with a setup including high speed cameras and a MCB as well.

7 Results and Discussion

7.1 Simple shapes

After a successful calibration, the next step was the investigation of the three-dimensional reconstruction of simple shapes as cube, cylinder, or prism. Furthermore, the dependency of the quality of the result and the angle between the cameras should be investigated as well. Figure 7.1 shows the setup for the first testing, including the two cameras, the tripods and a few possible test objects.



Fig. 7.1: Test setup

In order to investigate the angle dependency, the same setup as in Figure 7.1 was used. A rearrangement of both cameras has to be done to create a wide angle between them. As mentioned in section 5.3.3 it is important to recalibrate the system before taking new pictures. Figure 7.2 displays both taken images:

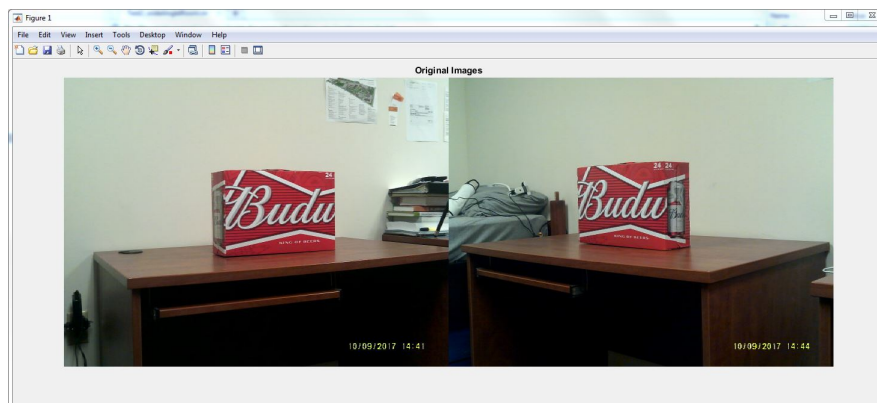


Fig. 7.2: Images for a wide angle test

After execution of all steps from section 5.4 the evaluation provided the following results, shown in Figure 7.3

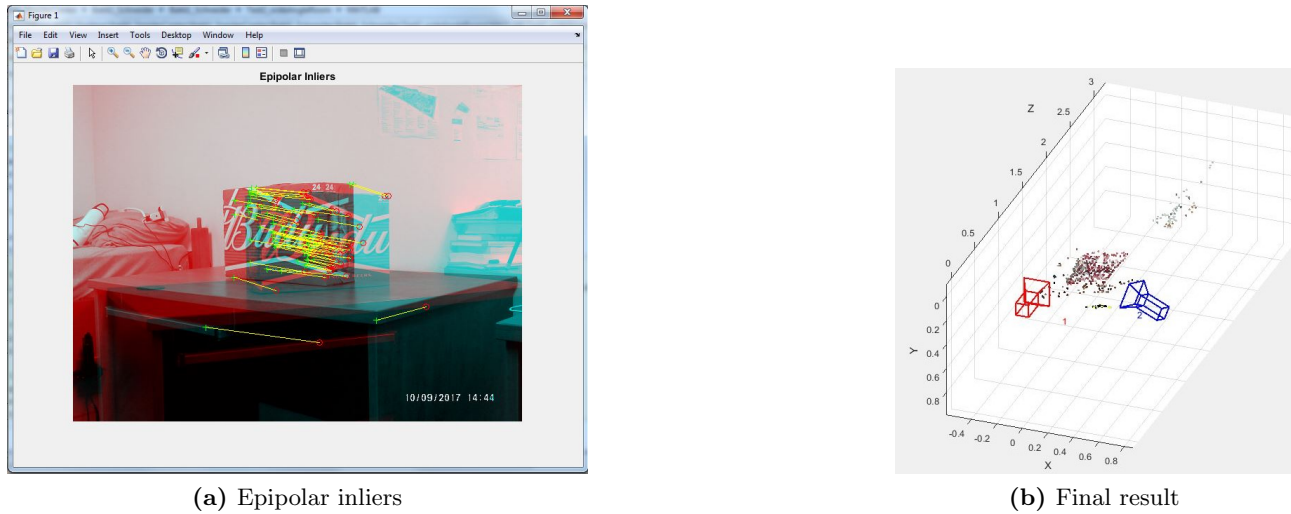


Fig. 7.3: Three dimensional reconstruction with the wide angle setup

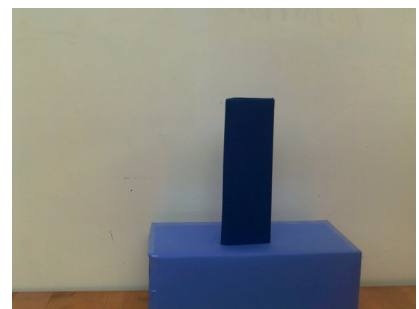
Figure 7.3a illustrates, that the algorithm was still able to detect corners, but the tracker obtained some errors during the point mapping. However, the final three dimensional reconstruction in Figure 7.3b is not useful. With a rising angle α , the number of similar points in the picture decreases, which means that the angle between the cameras should be set as narrow.

7.2 Covered simple shapes

The next step after applying the algorithm to create a satisfying result in terms of three dimensional reconstruction was to cover the test objects to obtain the actual contour of the test object instead of surface features. The two test objects were a prism on a cuboid box and a cube, as shown in Figure 7.4.



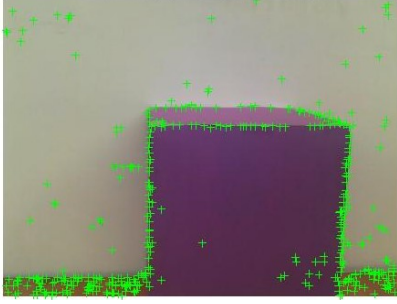
(a) Cube



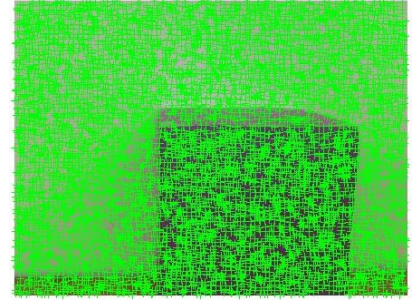
(b) Prism on a cuboid

Fig. 7.4: Test objects

At the beginning of the reconstruction process it is important to set the minimum accepted quality of corners detected. If the value is set to 0.01, MATLAB could only find 360 strongest corners in the image. Chose a value of 0.00002 leads to an amount of detected corners of 6526 including a lot of background or uninteresting points. Comparison between both settings is displayed in Figure 7.5.



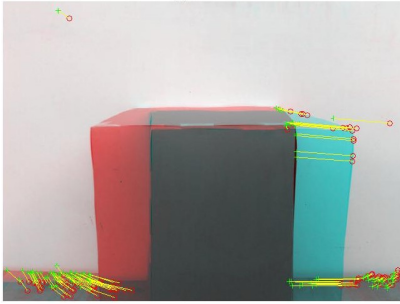
(a) 360 detected corners



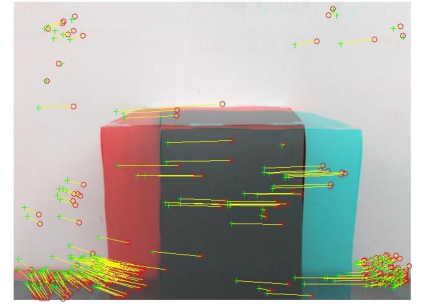
(b) 6526 detected corners

Fig. 7.5: value change of minimum accepted quality of corners

If the number of detected corners increases, the number of Epipolar inliers rises as well. In Figure 7.6 the different results of Epipolar inliers are clearly visible, Figure 7.6b contains more uninteresting background points:



(a) Epipolar inliers corresponding to 360 detected corners



(b) Epipolar inliers corresponding to 6526 detected corners

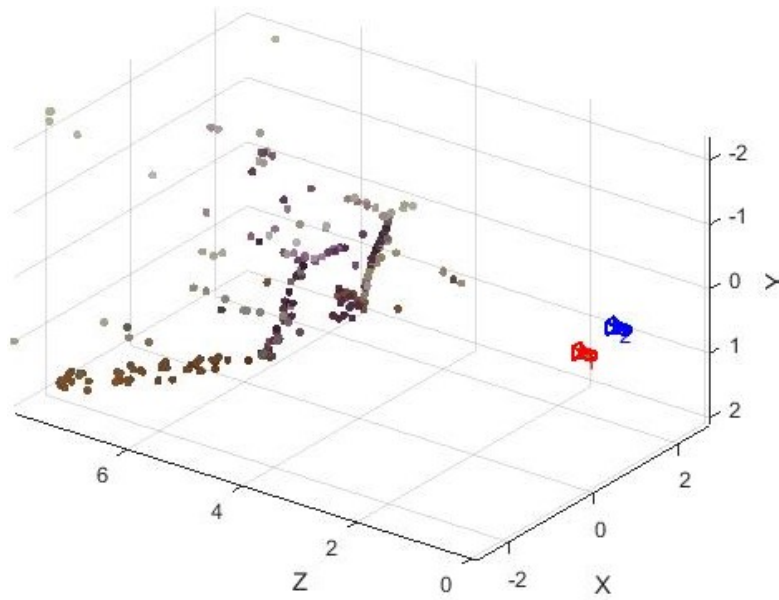
Fig. 7.6: Epipolar inliers

After executing the rest of the code, the two final point clouds were created. As mentioned before, a lower value of detected corners leads only to the outlines of the total cube. The second result provided more details about the shape in comparison to the first result, but the high number of background points is irritating. Both final results are displayed in Figure 7.7. The three dimensional reconstruction of the prism on a cuboid (see Figure 7.4b) was similar to the outcome described in Figure 7.7. Therefore, the final result of the second test object will not be discussed in detail.

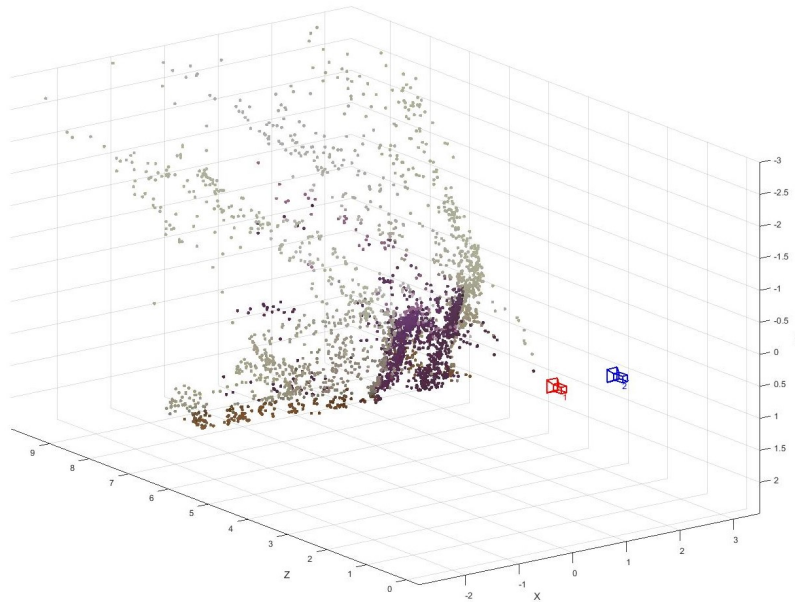
7.3 Complex shapes

As already mentioned, the purpose of this project is the investigation of electric arcs and their expansion. Therefore, a setup with more complex shapes is needed. A simple approximation to an electric arc is a branch. The setup is shown in Figure 7.8:

To minimize the detection of irritating points, a whiteboard with a sheet of paper was arranged in the background of the branch. Figure 7.9a shows the result of the corner detection, which is very accurate in the area of the white background paper. The detected points were covering the outline of



(a) Final result corresponding to 360 detected corners



(b) Final result corresponding to 6526 detected corners

Fig. 7.7: Final results

the limb. This result was expected, because the contrast of the dark limb in front of the white sheet is very high. Corner detection from an image of a real arc should provide a similar result, because high speed images of arcs are having a high contrast as well. Figure 7.9b illustrates the tracked features of the complex shape. Most of the detected corners were found correctly in the second image, just a few outliers were discernible.

After using the MATLAB "estimateEssentialMatrix" Function, the Epipolar inliers are displayed in Figure 7.10. The result indicates a lot of matched points above the actual contour. For a better reconstruction result, the minimum accepted quality of detected points was set to a lower value. As a side effect, MATLAB detected more corner points above the sheet of paper, because the whiteboard in the background was not perfectly clean. Finally, after all computational errors in the point cloud

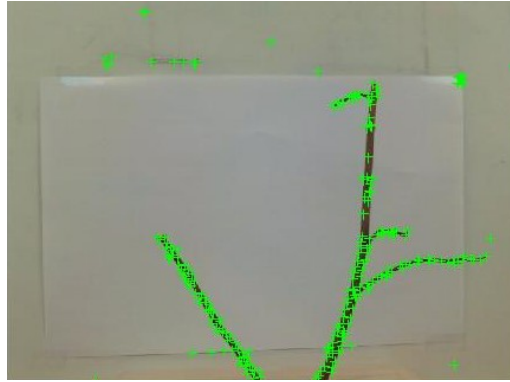


Fig. 7.8: Test setup for reconstruction of a complex shape

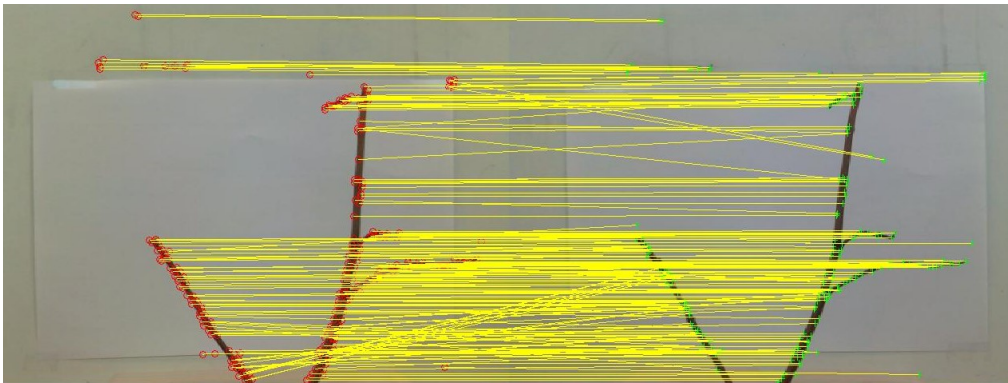
were removed through the filter, the three dimensional plot of the complex shape could be executed and is shown in Figure 7.11:

Figure 7.11a and Figure 7.11b show a comparison between the results with a change in the minimum accepted quality of detected corners. The complex shape of the limb is discernible in both Figures, but Figure 7.11a is obvious the more detailed reconstruction. A disadvantage is the high amount of irritating background points. A solution could be a color controlled filter, set individually depending on the colour range which should be removed from the reconstruction. Figure 7.11b includes less points, but it is enough to see the expansion of the complex structure in all directions.

It is possible to observe the three dimensional point cloud data plot in MATLAB from any desired angle. Two example views are shown in figure 7.12. The side view in Figure 7.12a is helpful to investigate the progress of the complex shape in the z axis, the front view in Figure 7.12b is showing x and y expansions.



(a) Detected corners



(b) Tracked features of the limb

Fig. 7.9: Detected corners and tracked features of a complex shape

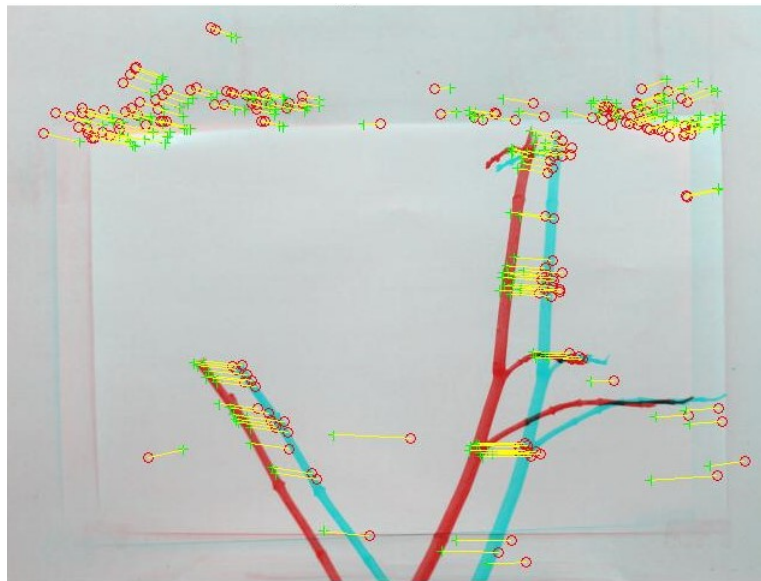
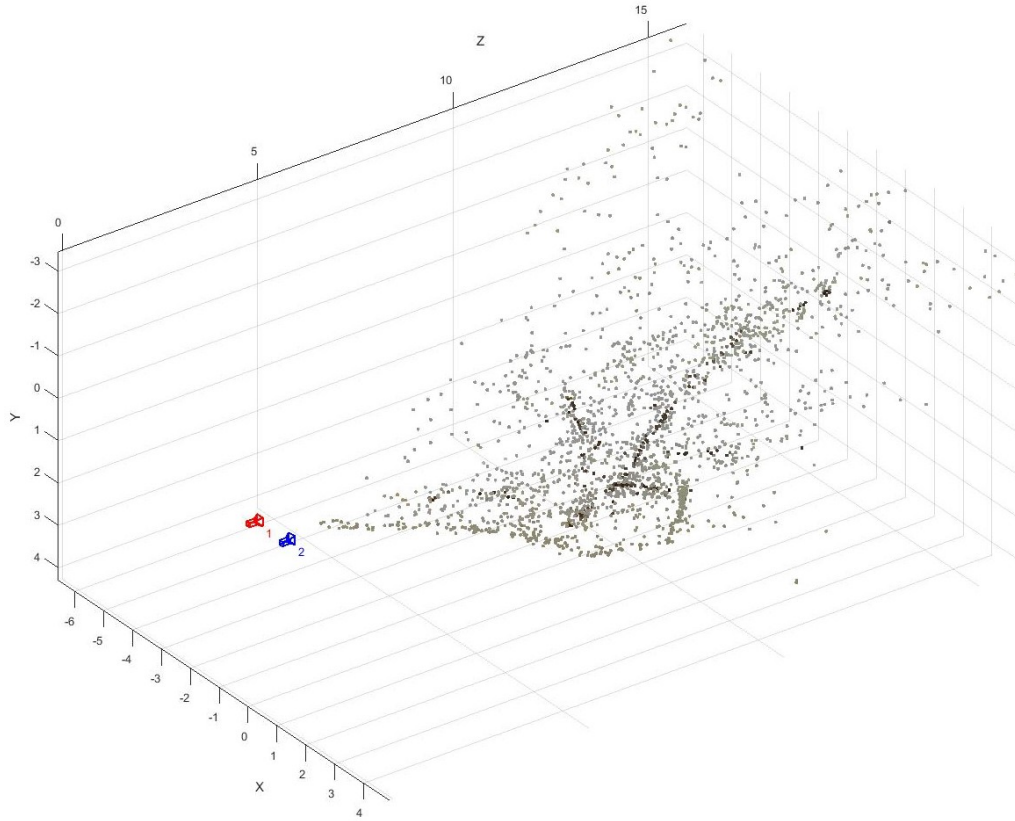
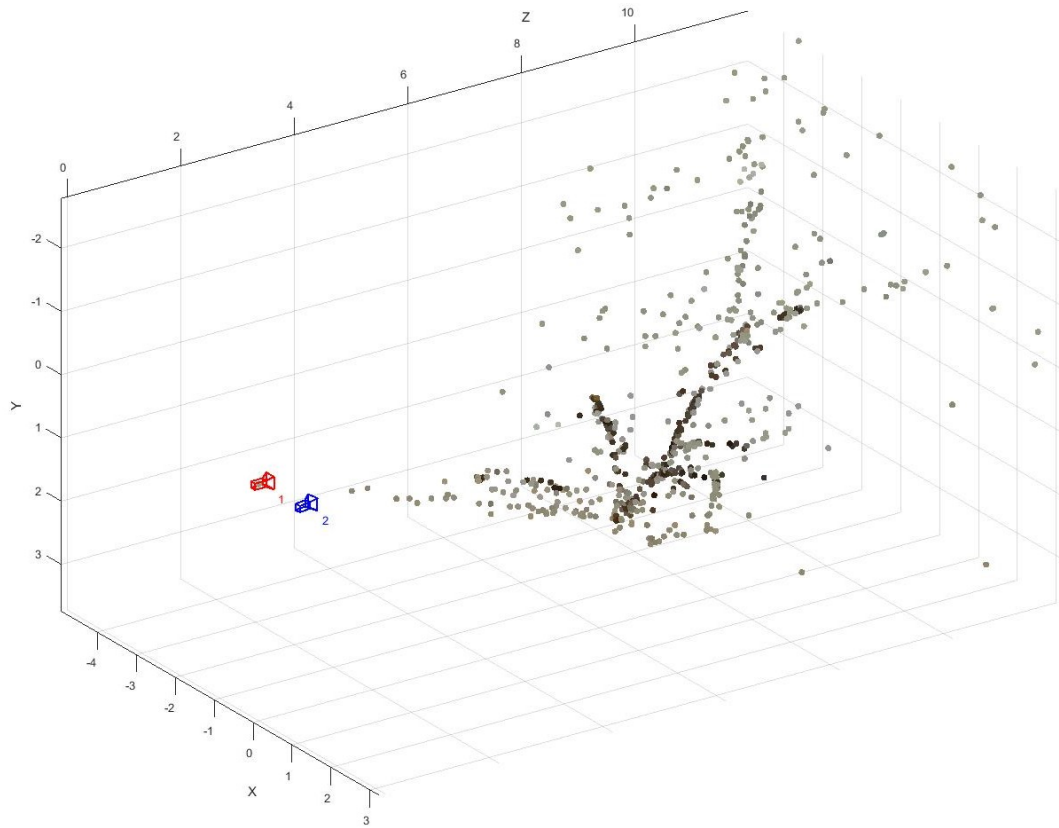


Fig. 7.10: Epipolar inliers

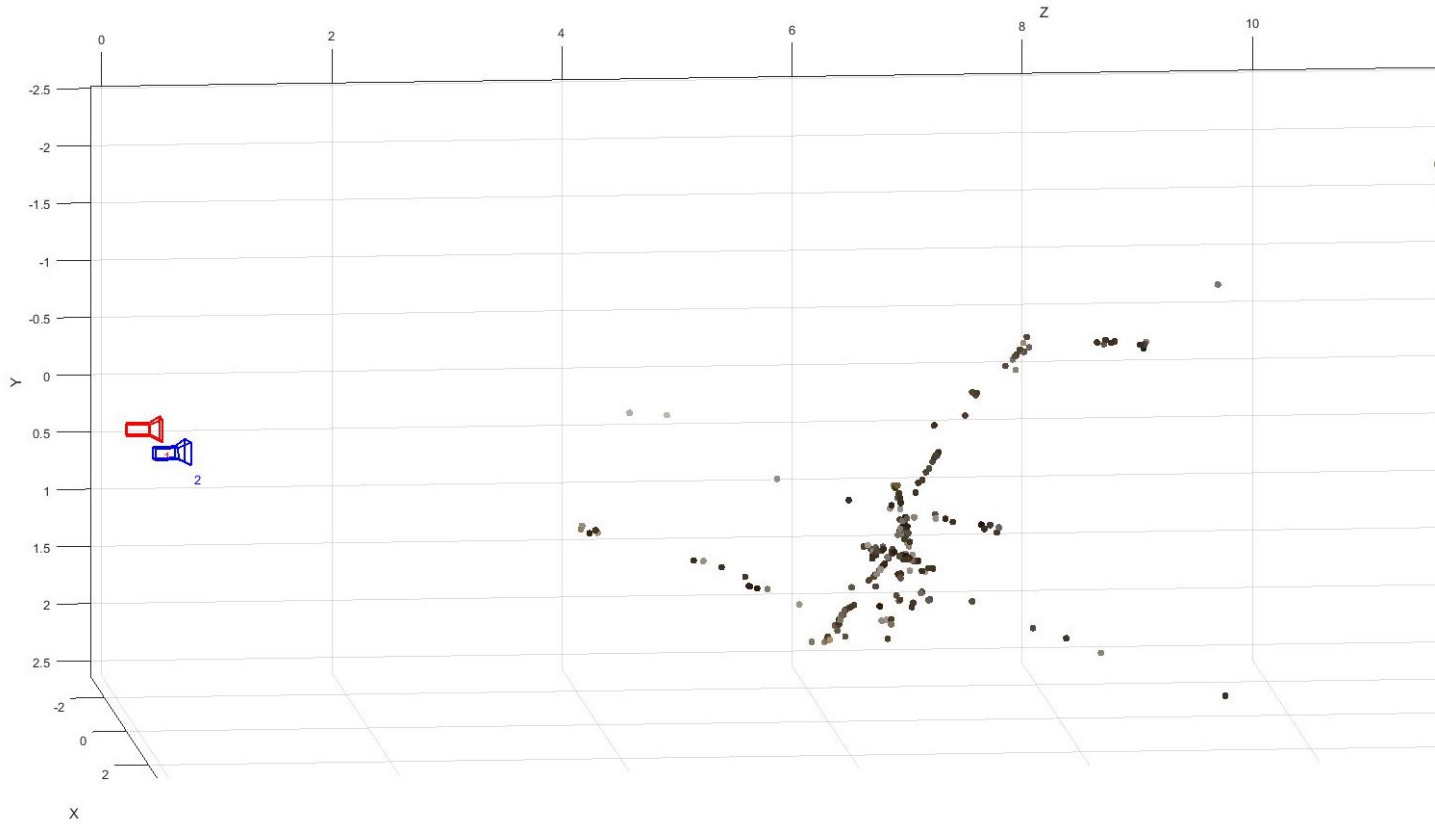


(a) High minimum accepted quality of corners

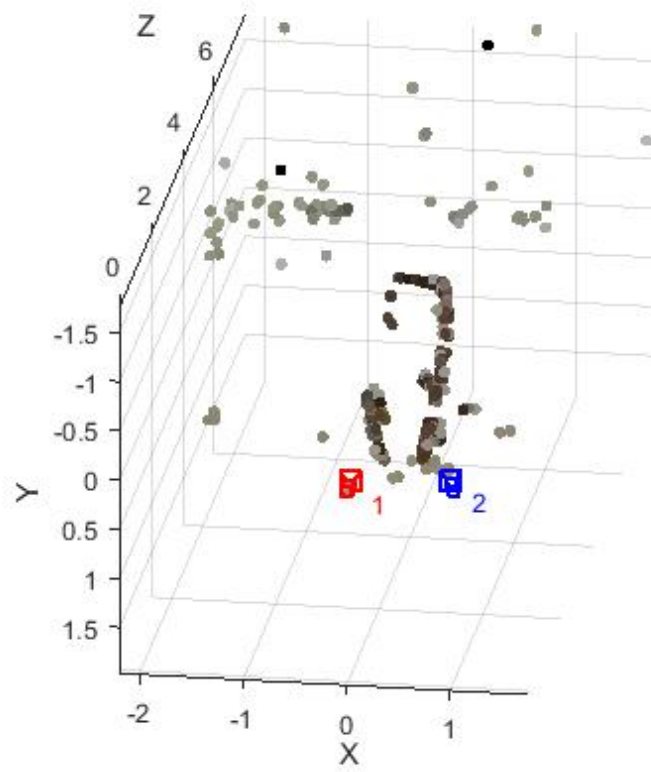


(b) Low minimum accepted quality of corners

Fig. 7.11: Comparison between high and low value of detected corners



(a) Side view



(b) Front view

Fig. 7.12: Different views of reconstruction result

8 Conclusion

This work presents a concept for a setup to generate a three dimensional image of an electric arc, recorded in a miniature circuit breaker by two CCD high speed cameras. In order to create such a setup, a theoretical research of existing state of the art systems was done. Furthermore, the research for a possible way to generate a three dimensional reconstruction out of two synchronous captured images was done as well. The next step was the selection of an appropriate software to implement the calibration and reconstruction process. After that, it was necessary to gain the knowledge to understand the provided apps and functions by MATLAB. To verify the functionality of the theoretical procedure, a few simple experiments were done. During these experiments, two different kinds of issues occurred. In order to provide a good quality of the final point cloud, computational errors were removed by a outlier point filter. To solve the problem of a high value of irritating background points, a color controlled filter was proposed in this work. Another investigated issue was the influence of the camera angle α onto the final result. In comparison to a wide angle α , a narrow angle provided satisfying results. The last series of tests was about the reconstruction of arc similar complex shapes. Section 7.3 illustrates satisfying reconstruction results, but in order to achieve different goals in terms of different resolution, scaling, three dimensional particle tracking and atmospheric discharges, future work needs to be done which is described in chapter 9.

9 Future Work

9.1 Different resolution

One of the main assumptions in this work was the equal resolution of all captured pictures (640x480 pixels). This was the lowest possible resolution for the taken pictures by the digital cameras. A high speed CCD camera is operating at a frame rate of more than 25 million frames per second (fps) [13]. For such a high frame rate, the resolution is decreasing to a few pixels. Therefore, a compromise between resolution and fps has to be found, because the quality of the three dimensional reconstruction result is decreasing for images with low resolution as well. However, the fact of different resolutions of the recordings provided by the high speed cameras has to be handled by the reconstruction algorithm. In order to use the setup described in chapter 5 (Figure 5.1) with two or more cameras with different resolutions, all images have to be adjusted to the image with the lowest resolution.

9.2 Reconstruction of high resolution images

This work is only using low resolution images, because of the reference to CCD high speed cameras and their high frame rate (detailed description in section 9.1). Nevertheless, high resolution images would end in a better three dimensional reconstruction result, because a higher resolution means a higher number of pixels. Therefore, edges and transitions are displayed more detailed in the image itself which leads to a better three dimensional reconstruction result in terms of accuracy.

9.3 Scaling

As mentioned in chapter 5.4, the three dimensional reconstruction result is an accurate reproduction from the real object up to a certain scale factor. In order to obtain exact dimensions from the final result, the scale factor has to be determined. One possible approach could be the implementation of reference objects with known dimensions in the final three dimensional reconstruction plot. The scale factor can be calculated by comparing the predefined size of the reference object with the measured size in the reconstruction plot. Once the factor is determined, exact measurements out of the final reconstruction result could be done.

9.3.1 Reference objects

Appropriate reference objects for the scaling method described in section 9.3 could be a sphere, a cube or any other simple geometric object.

9.4 High speed 3D-Particle tracking

High speed particle tracking is a method to track any particles that are present in fluids or gases. It is a Lagrangian approach, because particular particles are tracked.

The setup for a three dimensional particle tracking includes usually three or four cameras, circular arranged around the considered flow. These cameras have to be fully synchronized and are filming the diffracted or fluorescent light provided by the flow tracers. The flow itself has to be illuminated by a source of light (i.e. a collimated laser beam) There are no special requirements on the light source (coherent or monochromatic), as long as the observational volume is illuminated. For the best tracking result, as many cameras as possible should record the scene and track the fluorescent or diffractive particles or tracers. Basically, two cameras are sufficient to determine the exact three dimensional position of a particle, but the quality of the result would be better with more cameras respectively more captures images. Sometimes it is necessary to use three or more cameras to increase the accuracy of the final result. [14] Applied to a high speed setup recording an electric arc in a MCB, the particle movement in plasma jets could be tracked and displayed. However, perhaps a forecast regarding to the expansion and movement of an electric arc could be done based on this technique.

9.5 Atmospheric Discharges

Another application for three dimensional high speed filming could be the investigation of atmospheric discharges. Basically, the setup remains unchanged in terms of the required hardware. The only significant difference to the proposed system in this work would be the big distance between the lightning and the cameras. However, two or more high speed cameras are recording a thunderstorm from different points of view (i.e. on top of two mountains) and MATLAB could provide a complete reconstructed three dimensional image of a lightning. The outcome could be helpful for the investigation of thunderstorms, especially the expansion of lightnings and the location of lightning strikes. Unfortunately, the calibration and synchronisation of the cameras for such a setup could be difficult, because of the big distance between the object and the cameras.

9.5.1 Calibration

The calibration process for this work was done by taking pictures of a calibration pattern (chessboard) with known dimensions. (detailed description in section 5.3) Unfortunately, this calibration technique is inappropriate for a setup to investigate atmospheric discharges. (see section 9.5) For an exact working system, a new calibration method has to be developed. A possible way to calibrate could be the detection of a certain checkpoint (in example a clock tower, a mountaintop,...). The final accuracy of the setup after such a calibration is surely less than a small scale calibration in a laboratory test, but probably good enough to derive a satisfying final reconstruction of an lightning.

9.5.2 Synchronization

To guarantee a well working three dimensional reconstruction process, the images of all cameras have to be captured in the exact same moment (see chapter 5). Therefore, the system has to be fully

synchronized. The synchronization of a setup to capture images of atmospheric discharges could lead to a serious problem. One way to synchronize two or more cameras with great distance between them could be performed by the application of GPS time. This sort of timing could ensure an exactly coordinated setup in terms of synchronous recording time.

10 List of figures

1.1	Arc chute principles [1]	1
1.2	Basic electric circuit with a switch [1]	1
1.3	No counteracting voltage [1]	2
1.4	Counteracting voltage [1]	2
1.5	Two dimensional image of an electric arc [4]	3
2.1	Relationship between P(real World Point) and p (mapping on the projective Plane) [5]	4
2.2	Two examples for a Pinhole Camera Model [7], [8]	5
2.3	World coordinate system (W) and camera coordinate system (C) [5]	5
2.4	Epipolar geometry [6]	8
2.5	Triangulation method [5]	9
5.1	Possible final setup	13
5.2	Digital camera Polaroid is048	14
5.3	Test setup during calibration process with pattern	15
5.4	MATLAB Stereo Camera Calibration App	16
5.5	Camera and calibration pattern	16
5.6	Calibration App with imported pattern images	17
5.7	Different types of radial distortion [11]	17
5.8	Tangential distortion [11]	18
5.9	Skew factor [11]	18
5.10	Calibration Results after first computation	19
5.11	Calibration Results final computation and a certain tolerance of accuracy	19
5.12	Comparison between real and reconstructed scene based on calibration data	20
5.13	Detected cornes using the minimum eigenvalue algorithm by Shi and Tomasi	21
5.14	Tracked pointes by the KLT algorithm in a 'montage' plot	22
5.15	Epipolar inliers	22
5.16	Computation errors after triangulation	23
5.17	Three dimensional reconstruction result	24
7.1	Test setup	27
7.2	Images for a wide angle test	27
7.3	Three dimensional reconstruction with the wide angle setup	28
7.4	Test objects	28
7.5	value change of minimum accepted quality of corners	29
7.6	Epipolar inliers	29
7.7	Final results	30

7.8	Test setup for reconstruction of a complex shape	31
7.9	Detected corners and tracked features of a complex shape	32
7.10	Epipolar inliers	32
7.11	Comparison between high and low value of detected corners	33
7.12	Different views of reconstruction result	34

11 Bibliography

- [1] Peter Zeller. Components of Electrical Systems, Electrical Switches: Introductory Remarks and Basics.
- [2] Kirchhoff's circuit laws, January 2018. Page Version ID: 820355724.
- [3] Qian Wang. *Advanced Optical and 3D Reconstruction Diagnostics for Combustion and Fluids Research*. phd, University of Sheffield, January 2012.
- [4] Peter Zeller. Components of Electrical Systems, The electrical Arc.
- [5] Boguslaw Cyganek and J. Paul Siebert. *An Introduction to 3D Computer Vision Techniques and Algorithms*. John Wiley & Sons, August 2011. Google-Books-ID: 4leU0ZBkHngC.
- [6] Thesis: Stereo Imaging of The Dynamic Ignition of Flames in Gas Turbine - Mahmoud Abdul-Latif Assad - HQSF.
- [7] Pinhole camera model, January 2018. Page Version ID: 821304122.
- [8] Scratchapixel. 3d Viewing: the Pinhole Camera Model.
- [9] Z. Zhang. A flexible new technique for camera calibration. *IEEE Transactions on Pattern Analysis and Machine Intelligence*, 22(11):1330–1334, November 2000.
- [10] W. E. Grimson. Why Stereo Vision is Not Always about 3d Reconstruction. Technical Report AIM-1435, MASSACHUSETTS INST OF TECH CAMBRIDGE ARTIFICIAL INTELLIGENCE LAB, MASSACHUSETTS INST OF TECH CAMBRIDGE ARTIFICIAL INTELLIGENCE LAB, July 1993.
- [11] What Is Camera Calibration? - MATLAB & Simulink - MathWorks Deutschland.
- [12] MathWorks – Entwickler von MATLAB und Simulink.
- [13] High-speed camera, October 2017. Page Version ID: 806432391.
- [14] Particle tracking velocimetry, December 2017. Page Version ID: 813559348.